UVA Course on Accelerator Physics

SRF FOR ACCELERATORS

- BASICS -

Jean Delayen

Thomas Jefferson National Accelerator Facility

24 April 2006

Perfect Conductivity

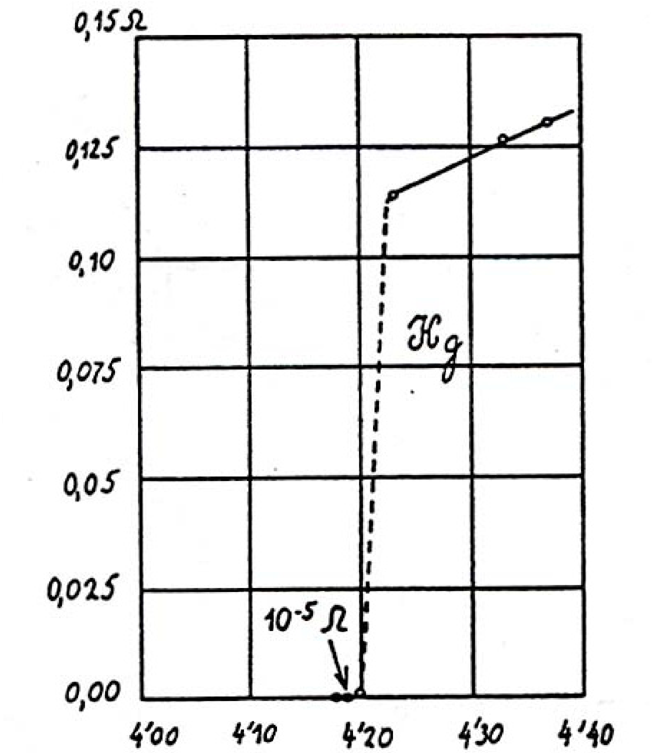

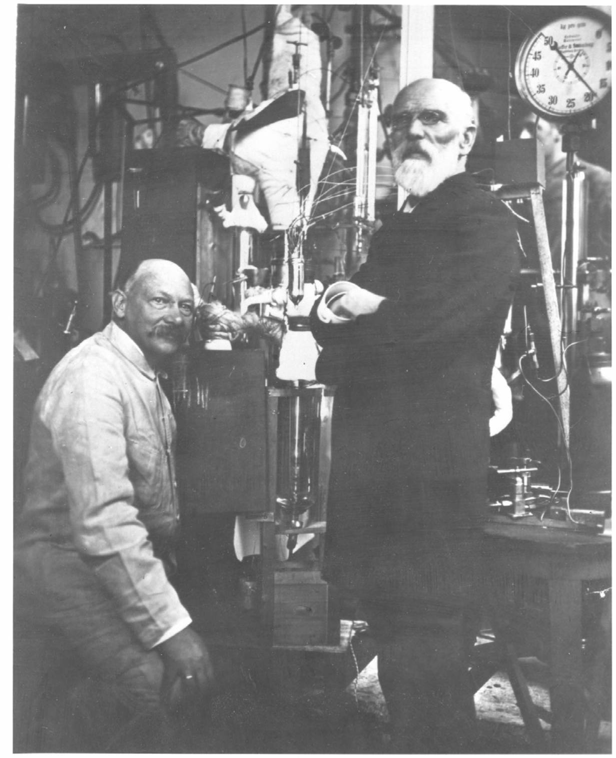

Kamerlingh Onnes and van der Waals in Leiden with the helium 'liquefactor' (1908)

Unexpected result

Expectation was the opposite: everything should become an isolator at $T \to 0$

Perfect Conductivity

Persistent current experiments on rings have measured

$$\frac{\sigma_s}{\sigma_n} > 10^{15}$$

Perfect conductivity is not superconductivity

A “perfect conductor” (infinite means free path, no scattering center) is not “resistance-less”

Perfect Diamagnetism

Perfect conductor

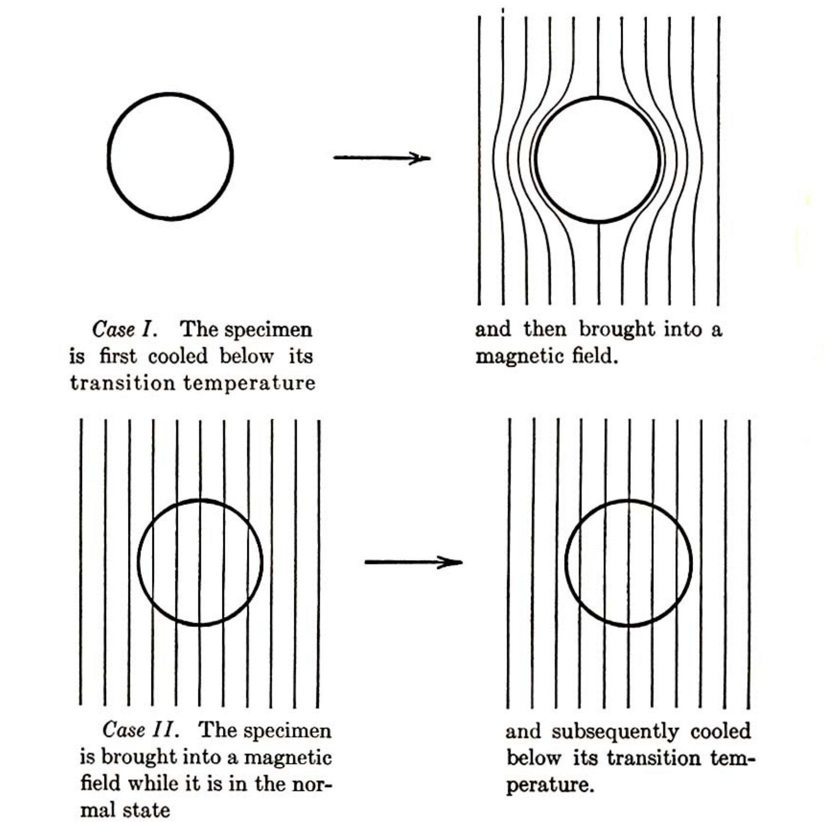

FIG. 3. The behavior expected for a transition into a state of *perfect conductivity*. The final state would depend on the *serial order* in which the specimen is brought into the same external conditions.

$$\frac{\partial B}{\partial t} = 0$$

Superconductor

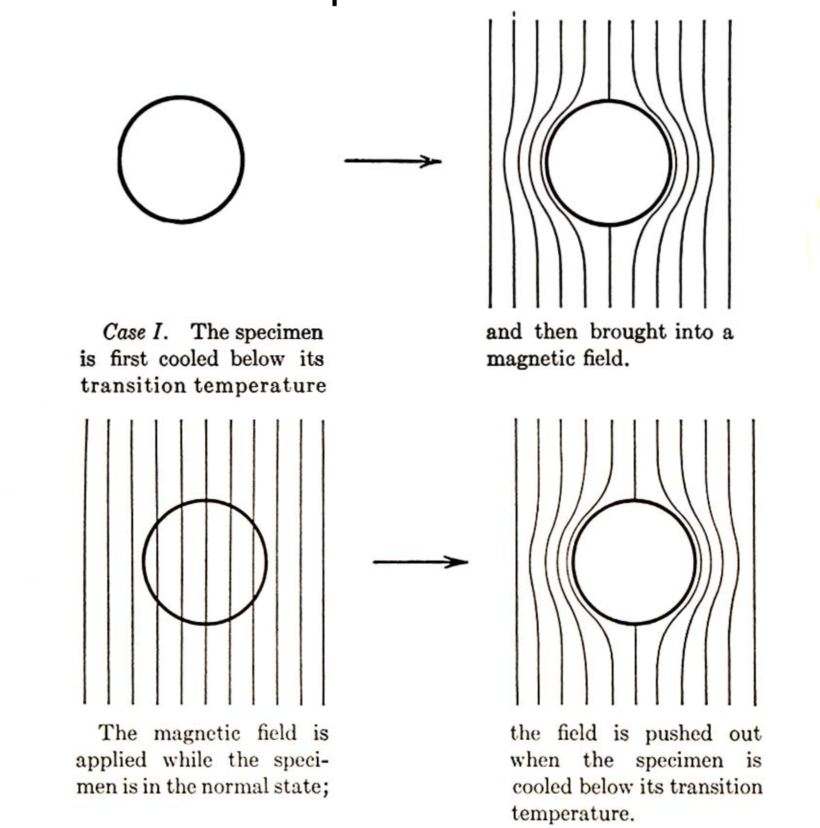

FIG. 4. Case II of Fig. 3 according to Meissner. The *superconductor*, in contrast to the perfect conductor, has zero magnetic induction independently of the way in which the superconducting state has been reached.

$$B = 0$$

Two Fluid Model – Gorter and Casimir

$T < T_c$ $\qquad x =$ fraction of "normal" electrons

$(1 - x)$: fraction of "condensed" electrons (zero entropy)

Assume: $\qquad \mathrm{F}(T) = x^{1/2}\,\mathrm{F_n}(T) + (1-x)\,\mathrm{F_s}(T) \qquad$ free energy

$$\mathrm{F_n}(T) = -\frac{1}{2}\gamma T^2$$

$$\mathrm{F_s}(T) = -\beta = -\frac{1}{4}\gamma T_c^2$$

Minimization of $\mathrm{F}(T)$ gives $\qquad x = \left(\frac{\mathrm{T}}{\mathrm{T_C}}\right)^4$

$$C_{es} = 3\gamma\frac{\mathrm{T}^3}{\mathrm{T_c^2}}$$

$$\frac{H_c(T)}{H_o} = 1 - \left(\frac{\mathrm{T}}{\mathrm{T_C}}\right)^2$$

Model of F & H London (1935)

Frictionless "superelectrons"

$$m\frac{\partial \vec{\upsilon}}{\partial t} = -e\vec{E} \qquad \overrightarrow{J_s} = -en_s\,\vec{\upsilon}$$

$$\frac{\partial \vec{J}_s}{\partial t} = \frac{n_s e^2}{m}\vec{E}$$

$$\text{Maxwell}: \ \vec{\nabla}\times\vec{E} = -\frac{\partial \vec{B}}{\partial t}$$

$$\Rightarrow \frac{\partial}{\partial t}\left(\frac{m}{n_s e^2}\vec{\nabla}\times\vec{\mathrm{J}}_{\mathrm{s}} + \vec{\mathrm{B}}\right) = 0 \qquad \Rightarrow \frac{m}{n_s e^2}\vec{\nabla}\times\vec{\mathrm{J}}_{\mathrm{s}} + \vec{\mathrm{B}} = \text{Constant}$$

$$\text{F \& H London}: \quad \frac{m}{n_s e^2}\vec{\nabla}\times\vec{\mathrm{J}}_{\mathrm{s}} + \vec{\mathrm{B}} = 0$$

Model of F & H London (1935)

combine with $\vec{\nabla} \times \vec{B} = \mu_o \vec{J}_s$

$$\boxed{\nabla^2 \vec{B} - \frac{\mu_0 n_s e^2}{m} \vec{B} = 0}$$

$$B(x) = B_o \exp\left[-x/\lambda_L\right]$$

$$\lambda_L = \left[\frac{m}{\mu_0 n_s e^2}\right]^{\frac{1}{2}}$$

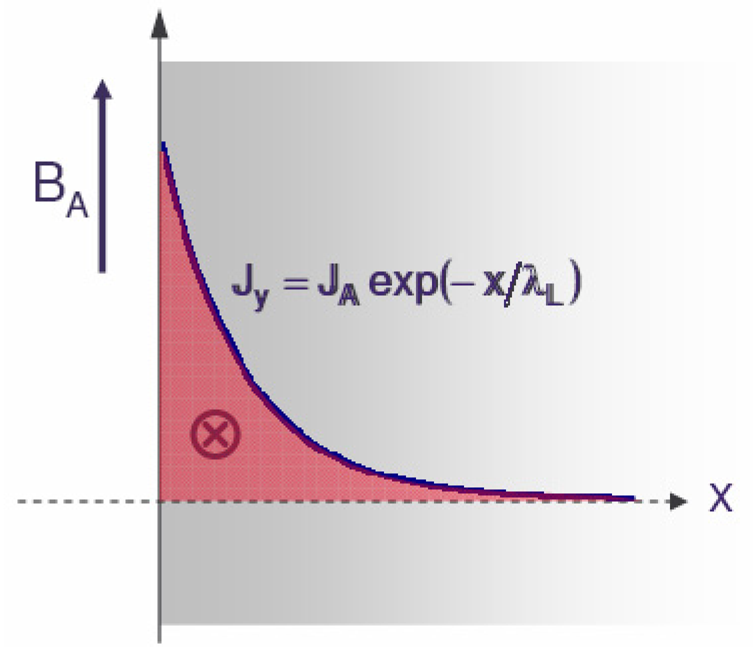

The magnetic field, and the current, decay exponentially over a distance λ (a few 10s of nm)

Model of F & H London (1935)

$$\lambda_L = \left[\frac{m}{\mu_0 n_s e^2}\right]^{\frac{1}{2}}$$

From Gorter and Casimir two-fluid model

$$n_s \propto \left[1-\left(\frac{T}{T_C}\right)^4\right]$$

$$\lambda_L(T) = \lambda_L(0)\frac{1}{\left[1-\left(\frac{T}{T_C}\right)^4\right]^{\frac{1}{2}}}$$

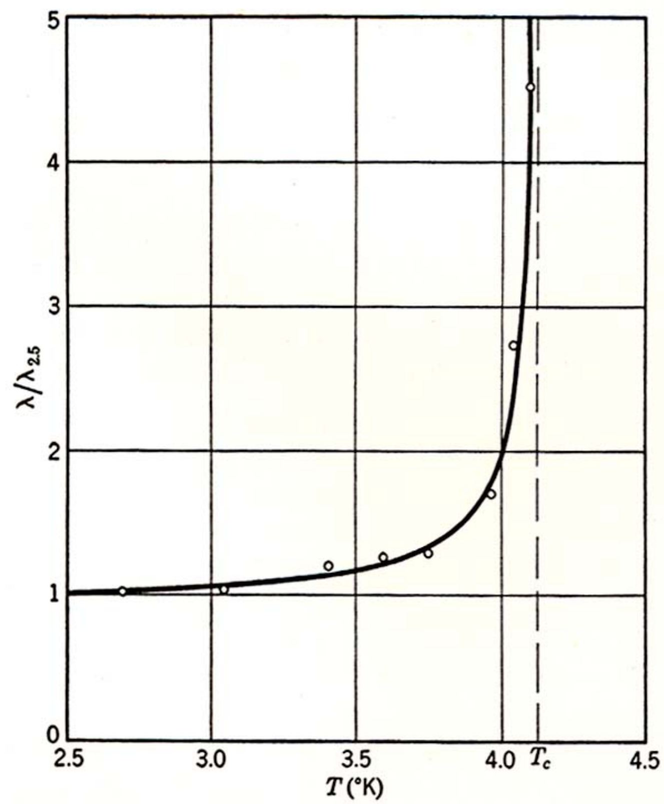

FIG. 21. Penetration depth as a function of temperature. (After Shoenberg, *Nature*, **43**, 433, 1939.)

Pippard's Extension of London's Model

Observations:

-Penetration depth increased with reduced mean free path

- H_c and T_c did not change

- Need for a positive surface energy over 10^{-4} cm to explain existence of normal and superconducting phase in intermediate state

Non-local modification of London equation

Local: $$\vec{J} = -\frac{1}{c\lambda}\vec{A}$$

Non local: $$\vec{J}(r) = -\frac{3}{4\pi\xi_0\lambda}\int \frac{\vec{R}\left[\vec{R}\bullet\vec{A}(r')\right]e^{-\frac{R}{\xi}}}{R^4}d\upsilon$$

$$\frac{1}{\xi} = \frac{1}{\xi_0} + \frac{1}{\ell}$$

Two Fundamental Lengths

- London penetration depth λ
  — Distance over which magnetic fields decay in superconductors

- Pippard coherence length ξ
  — Distance over which the superconducting state decays

Surface Energy

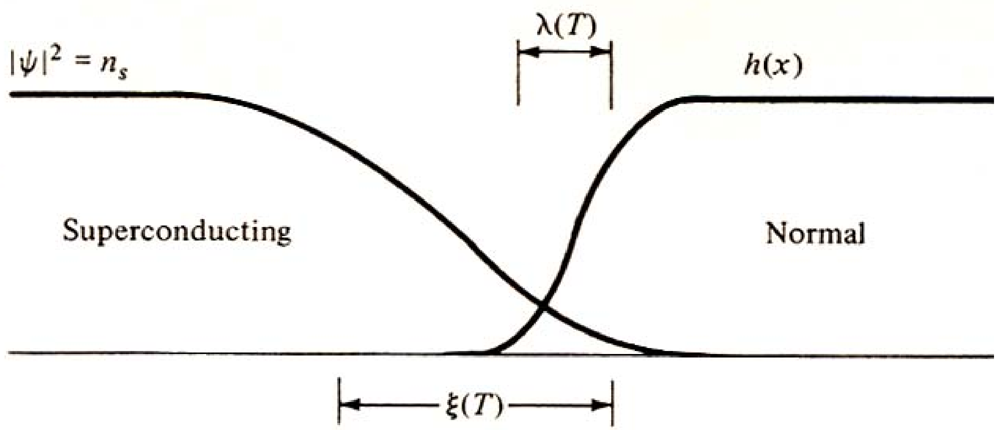

FIGURE 1-4
Interface between superconducting and normal domains in the intermediate sta

$$\sigma \simeq \frac{1}{8\pi}\left[H_c^2\xi - H^2\lambda\right]$$

$\frac{H^2\lambda}{8\pi}$: Energy that can be gained by letting the fields penetrate

$\frac{H_c^2\xi}{8\pi}$: Energy lost by "damaging" superconductor

Surface Energy

$$\sigma \simeq \frac{1}{8\pi}\left[H_c^2\xi - H^2\lambda\right]$$

Interface is stable if σ>0

If $\xi >> \lambda$ σ>0

Superconducting up to H_c where superconductivity is destroyed globally

If $\lambda >> \xi$ σ<0 for $H^2 > H_c^2 \dfrac{\xi}{\lambda}$

Advantageous to create small areas of normal state with large area to volume ratio → quantized fluxoids

Exact calculation:

$$\kappa = \frac{\lambda}{\xi} < \frac{1}{\sqrt{2}} \quad : \text{Type I}$$

$$\kappa = \frac{\lambda}{\xi} > \frac{1}{\sqrt{2}} \quad : \text{Type II}$$

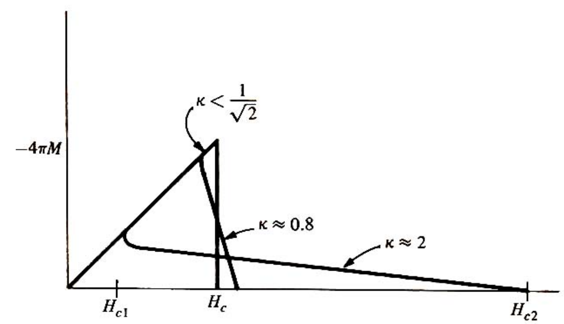

FIGURE 5-2
Comparison of magnetization curves for three superconductors with the same value of thermodynamic critical field H_c, but different values of κ. For $\kappa < 1/\sqrt{2}$, the superconductor is of type I and exhibits a first-order transition at H_c. For $\kappa > 1/\sqrt{2}$, the superconductor is type II and shows second-order transitions at H_{c1} and H_{c2} (for clarity, marked only for the highest κ case). In all cases, the area under the curve is the condensation energy $H_c^2/8\pi$.

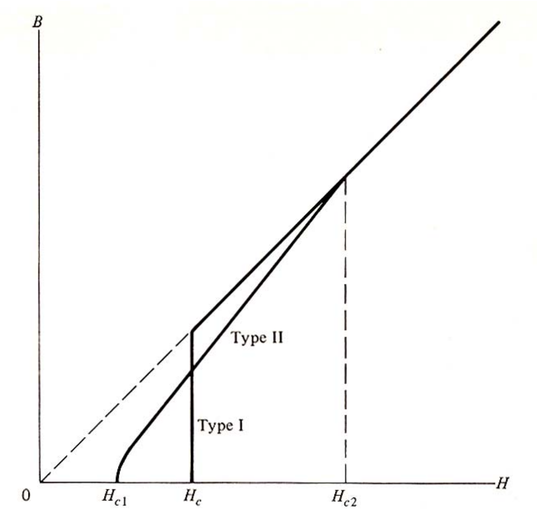

FIGURE 1-5
Comparison of flux penetration behavior of type I and type II superconductors with the same thermodynamic critical field H_c. $H_{c2} = \sqrt{2}\kappa H_c$. The ratio of B/H_{c2} from this plot also gives the approximate variation of R/R_n, where R is the electrical resistance for the case of negligible pinning, and R_n is the normal-state resistance.

Critical Fields

Type I $\quad H_c \quad$ Thermodynamic critical field

$$H_{sh} \simeq \frac{H_c}{\sqrt{\kappa}}$$ Superheating critical field

Field at which surface energy is 0

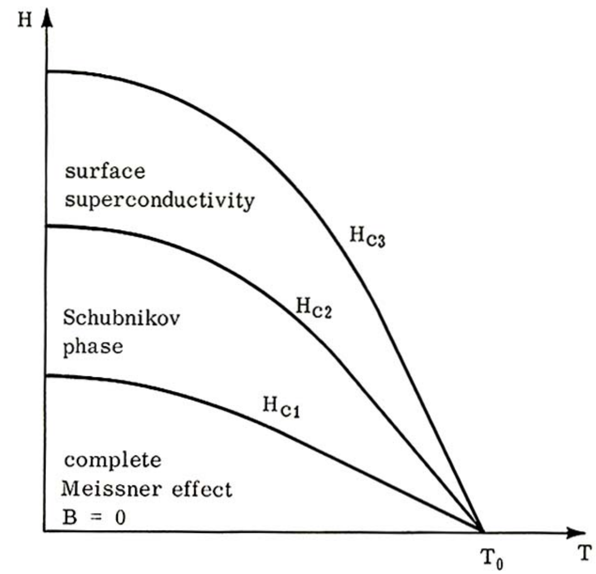

Figure 3-1
Phase diagram for a long cylinder of a Type II super-conductor.

Type II $\quad H_c \quad$ Thermodynamic critical field

$$H_{c1} \simeq \frac{H_c^2}{H_{c2}} < H_c$$

$$H_{c2} = \sqrt{2\kappa}\; H_c > H_c$$

Superheating Field

Ginsburg-Landau:

$$H_{sh} \sim \frac{0.9H_c}{\sqrt{\kappa}} \quad \text{for } \kappa \ll 1$$

$$\sim 1.2\ H_c \quad \text{for } \kappa \sim 1$$

$$\sim 0.75\ H_c \quad \text{for } \kappa \gg 1$$

The exact nature of the rf critical field of superconductors is still an open question

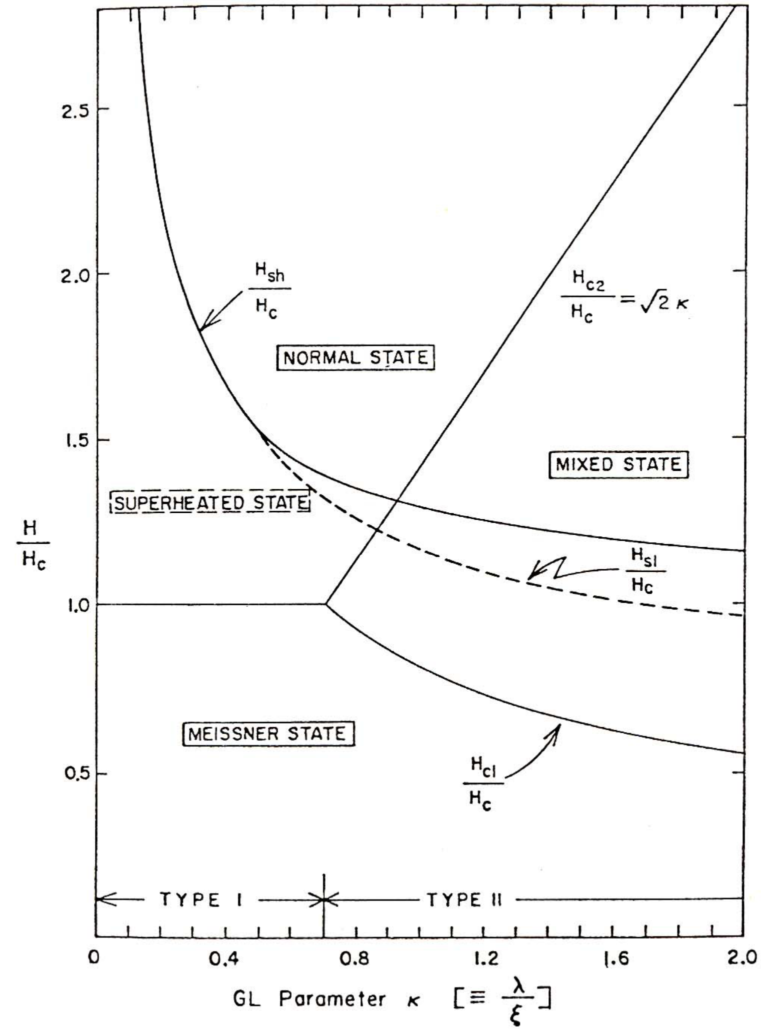

Fig. 13: Phase diagram of superconductors[42] in the transition regime of type I and II. The normalized critical fields are shown as a function of κ.

BCS

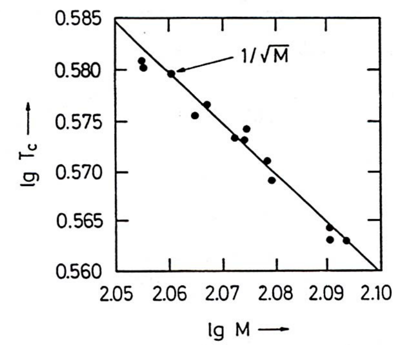

- – Energy gap
- –Isotope effect (phonons)
- –Meissner effect

Assumption: Phonon-mediated attraction between electron of equal and opposite momenta located within $\hbar\omega_D$ of Fermi surface

Moving electron distorts lattice and leaves behind a trail of positive charge that attracts another electron moving in opposite direction
Fermi ground state is unstable
Electron pairs can form bound states of lower energy

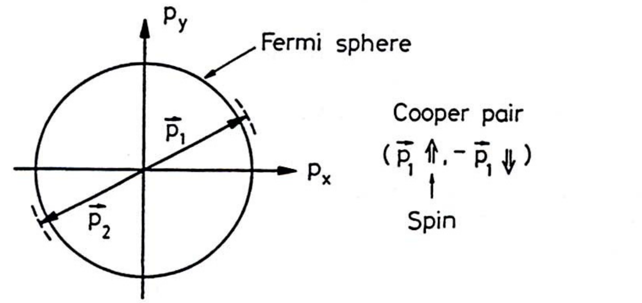

Figure 20: A pair of electrons of opposite momenta added to the full Fermi sphere.

BCS

Exchange of phonon between 2 electrons can lead to an attraction between them.

This attraction can lead electrons of opposite momenta to form pairs.

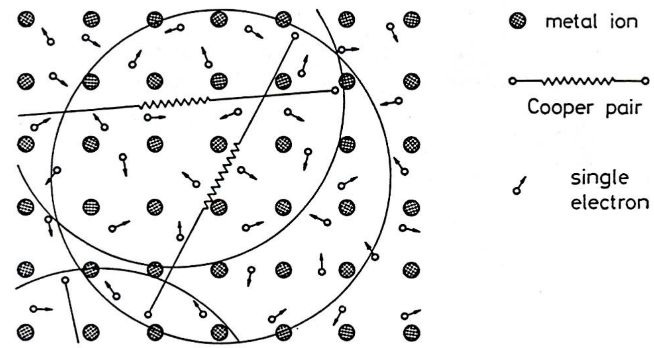

Figure 22: Cooper pairs and single electrons in the crystal lattice of a superconductor. (After Essmann and Träuble [12]).

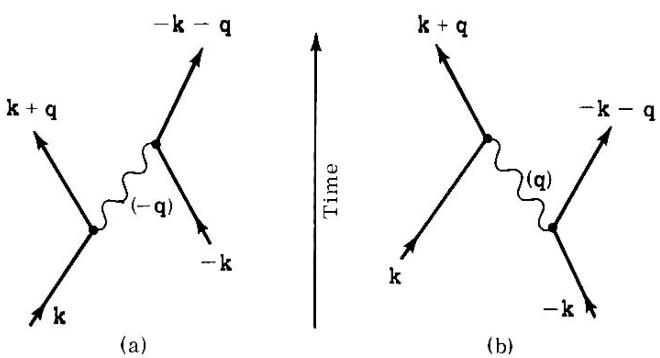

Figure 4-1

Electron-electron interaction via phonons. In process (a) the electron $\mathbf{k}$ emits a phonon of wave-vector $-\mathbf{q}$. The phonon is absorbed later by the second electron. In process (b) the second electron in state $(-\mathbf{k})$ emits a phonon $\mathbf{q}$, subsequently absorbed by the first electron.

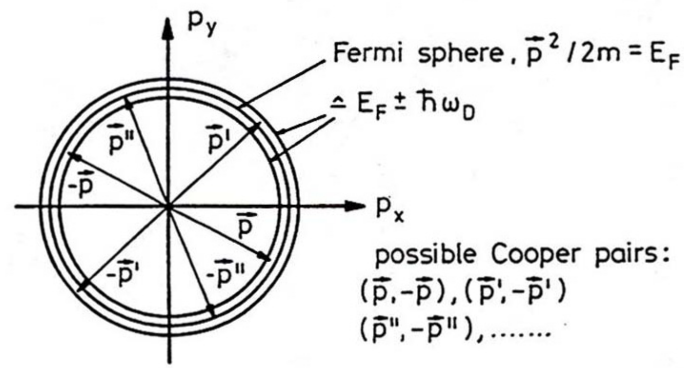

Figure 23: Various Cooper pairs $(\vec{p},-\vec{p})$, $(\vec{p}',-\vec{p}')$, $(\vec{p}'',-\vec{p}'')$, ... in momentum space.

BCS and BEC

BCS	BEC
weak coupling	strong coupling
large pair size **k**-space pairing	small pair size **r**-space pairing
strongly overlapping Cooper pairs	ideal gas of preformed pairs

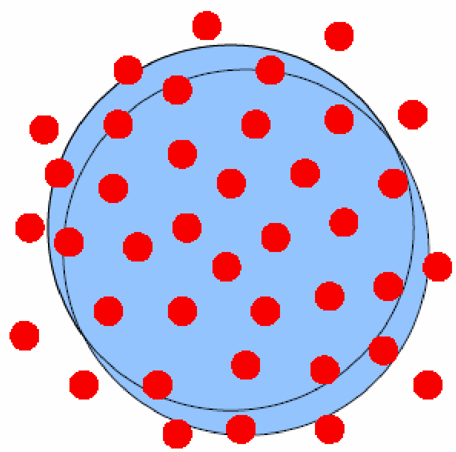

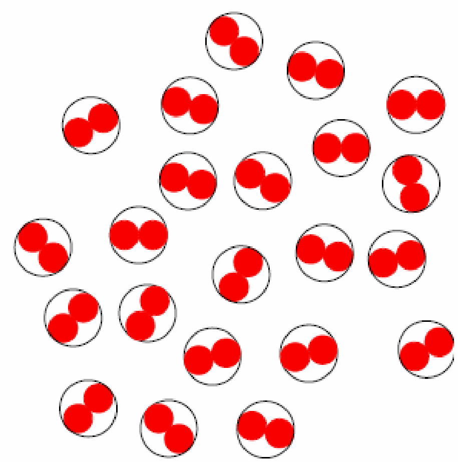

BCS

Energy gap

$$\Delta_0 = \frac{\hbar\omega_D}{\sinh\left[\frac{1}{\rho(0)V}\right]} \simeq 2\hbar\omega_D \, e^{-\frac{1}{\rho(0)V}}$$

Energy of excited states:

$$\varepsilon_k = 2\sqrt{\xi_k^2 + \Delta_0^2}$$

Condensation energy: $E_s - E_n = -\frac{\rho(0)V\Delta_0^2}{2}$

$$\simeq -N\Delta_0\left(\frac{\Delta_0}{\varepsilon_F}\right) = \frac{H_0^2}{8\pi}$$

$$\Delta_0 / k \simeq 10K$$

$$\varepsilon_F / k \simeq 10^4 K$$

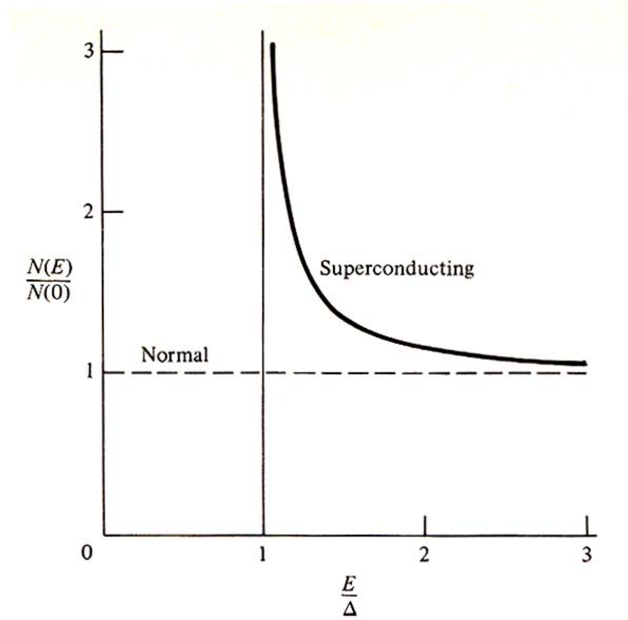

FIGURE 2-4
Density of states in superconducting compared to normal state. All **k** states whose energies fall in the gap in the normal metal are raised in energy above the gap in the superconducting state.

BCS

Temperature dependence of the energy gap

$$\frac{1}{V\rho(0)} = \int_0^{\hbar\omega_D} \frac{\tanh\left[\left(\varepsilon^2+\Delta^2\right)^{1/2}/2kT\right]}{\left(\varepsilon^2+\Delta^2\right)^{1/2}}\,d\varepsilon$$

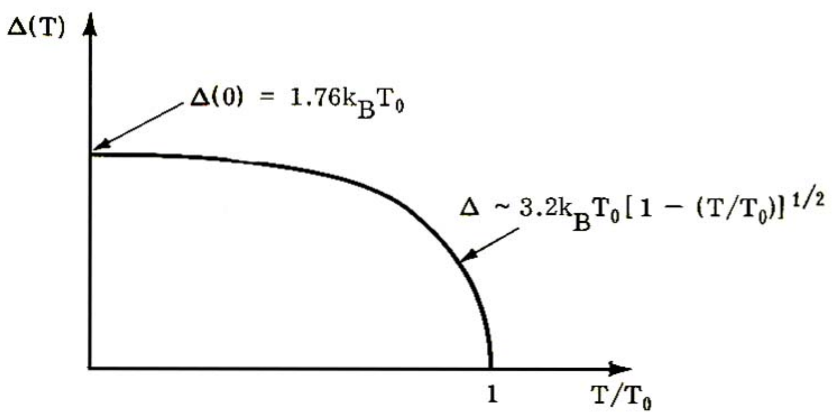

Figure 4-4
Variation of the order parameter Δ with temperature in the BCS approximation.

BCS

Critical temperature:

$$kT_c = 1.14\,\hbar\omega_D \quad \exp\left[-\frac{1}{VN(E_F)}\right]$$

$$\Delta(0) = 1.76\, kT_c$$

Heat capacity

$$C_{es} \simeq \exp\left(-\frac{\Delta}{kT}\right) \quad \text{for} \quad T < \frac{T_c}{10}$$

coherence length

$$\xi_0 = .18\frac{\hbar \upsilon_F}{kT_c}$$

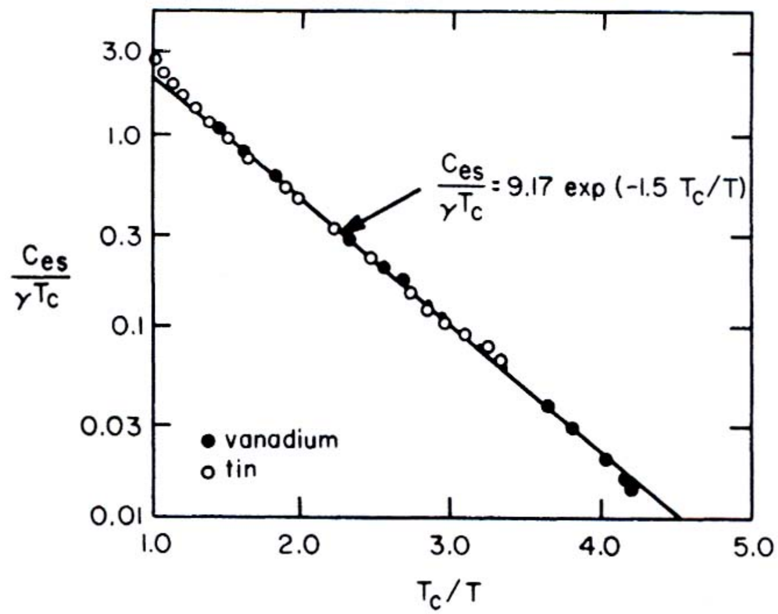

Fig. 22. Reduced electronic specific heat in superconducting vanadium and tin. [From Biondi et al., (*150*).]

Penetration Depth

$$\lambda = \frac{2}{\pi}\int \frac{dk}{K(k)+k^2}\,dk \qquad \text{(specular)}$$

Represented accurately by $\lambda \sim \dfrac{1}{\sqrt{1-\left(\dfrac{T_c}{T}\right)^4}}$ near T_c

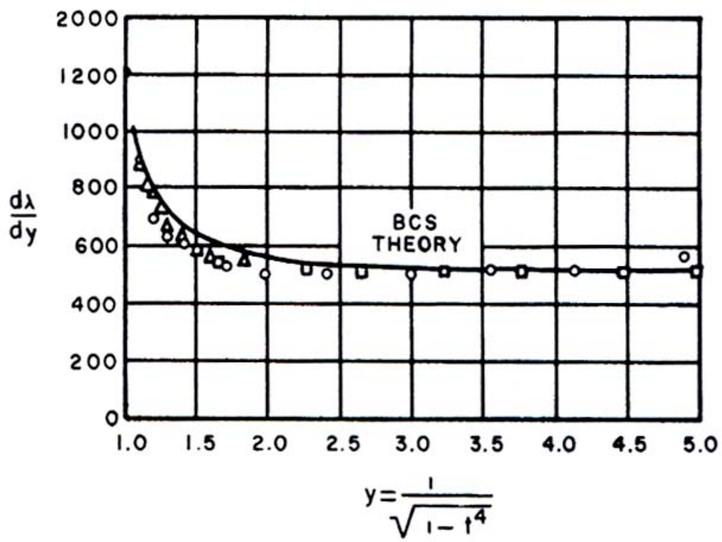

Fig. 30. Temperature dependence of $d\lambda/dy$ for tin obtained by Schawlow and Devlin (*207*) compared with the theoretical curve obtained from the BCS theory.

BCS Model

- The BCS model is an extremely simplified model of reality
  - The Coulomb interaction between single electrons is ignored
  - Only the term representing the scattering of pairs is retained
  - The interaction term is assumed to be constant over a thin layer at the Fermi surface and 0 everywhere else
  - The Fermi surface is assumed to be spherical

- Nevertheless, the BCS results (which include only a very few adjustable parameters) are amazingly close to the real world

Surface Impedance in the G-C-L Model

Time-varying magnetic field will create an electric field in the superconductor, that will interact with the "normal" electrons

$\longrightarrow$ Power dissipation

$$\vec{\nabla} \times \vec{E} = -\frac{\partial \vec{B}}{\partial t} \qquad \Rightarrow \qquad E \propto \lambda \omega H$$

$$\text{Losses} \quad \propto E^2 \lambda n \propto \omega^2 \lambda^3 n_n(t) \quad \propto \quad \omega^2 \frac{t^4}{\left(1-t^4\right)^{\frac{3}{2}}}$$

Close to T_c: R_s dominated by $\lambda(t)$

Far from T_c: R_s dominated by $n(t)$

Normal Conductors (local limit)

- In the local limit $\vec{J}(z) = \sigma \vec{E}(z)$
- The fields decay with a characteristic length (skin depth) $\delta = \left(\dfrac{2}{\mu_0 \omega \sigma}\right)^{1/2}$

$$E_x(z) = E_x(0) e^{-z/\delta} e^{-iz/\delta}$$

$$H_y(z) = \frac{(1-i)}{\mu_0 \omega \delta} E_x(z)$$

$$Z = \frac{E_x(0)}{H_y(0)} = \frac{(1+i)}{2} \mu_0 \omega \delta = \frac{(1+i)}{\sigma \delta} = (1+i)\left(\frac{\mu_0 \omega}{2\sigma}\right)^{1/2}$$

Electrodynamics and Surface Impedance in BCS Model

$$H_0\phi + H_{ex}\,\phi = i\hbar\frac{\partial\phi}{\partial t}$$

$$H_{ex} = \frac{e}{mc}\sum A(r_i,t)\,p_i$$

H_{ex} is treated as a small perturbation $\qquad H_{rf} << H_c$

There is, at present, no model for superconducting surface resistance at high rf field

$$J \propto \int \frac{R[R\cdot A]\,I(\omega,R,T)\,e^{-\frac{R}{l}}}{R^4}dr$$

similar to Pippard's model

$$J(k) = -\frac{c}{4\pi}K(k)A(k)$$

$K(0)\neq 0:$ Meissner effect

Surface Resistance of Superconductors

Temperature dependence

–close to T_c :

dominated by change in $\lambda(t) \quad \frac{t^4}{\left(1-t^2\right)^{3/2}}$

–for $T < \frac{T_c}{2}$:

dominated by density of excited states $\sim e^{-\Delta/kT}$

$$R_s \sim \frac{A}{T}\omega^2 \exp \quad -\frac{\Delta}{kT}$$

Frequency dependence

ω^2 is a good approximation

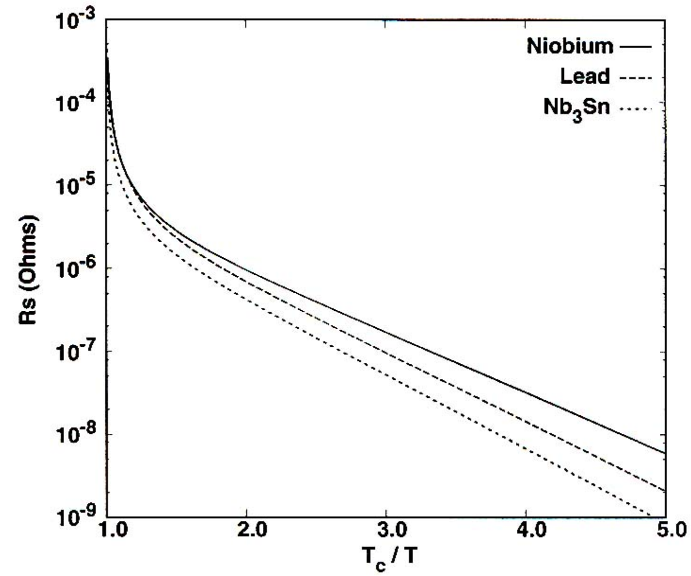

Figure 4.5: Theoretical surface resistance at 1.5 GHz of lead, niobium and Nb_3Sn as calculated from program [94]. The values given in Table 4.1 were used for the material parameters.

Surface Resistance of Superconductors

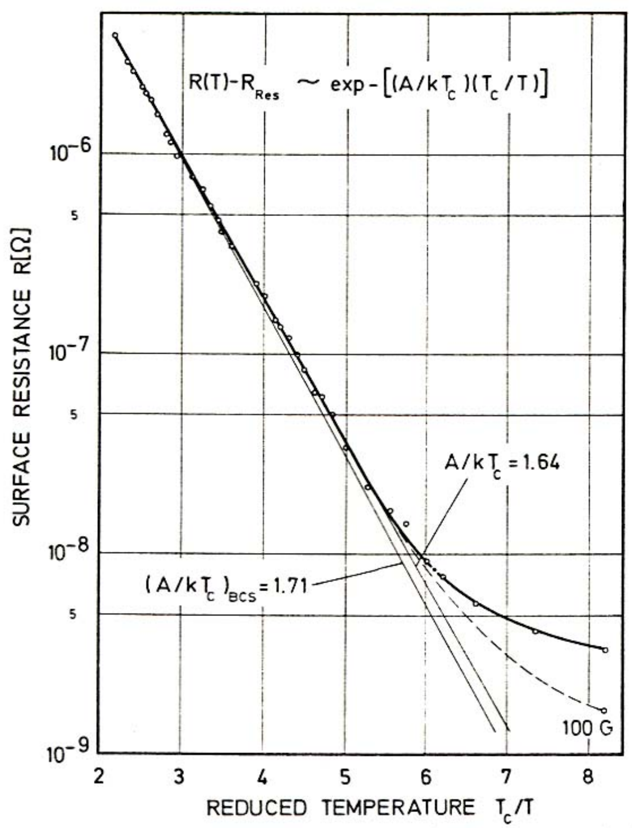

Fig. 2. Temperature dependence of surface resistance of niobium at 3.7 GHz measured in the TE_{011} mode at $H_{rf} \simeq 10$ G. The values computed with the BCS theory used the following material parameters:

$T_c = 9.25$ K; $\lambda_L(T=0, l=\infty) = 320$ Å;

$\Delta(0)/kT = 1.85$; $\xi_F(T=0, l=\infty) = 620$ Å; $l = 1000$ Å or 80 Å.

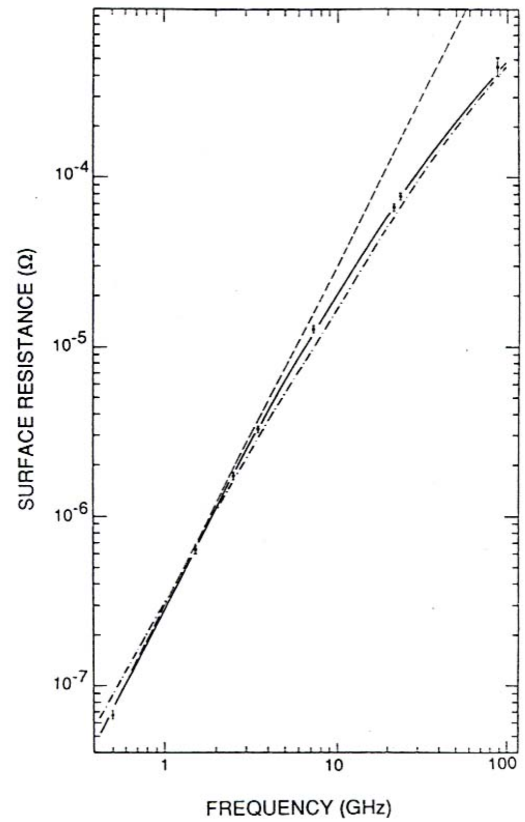

Fig. 5. The surface resistance of Nb at 4.2 K as a function of frequency [62,63]. Whereas the isotropic BCS surface resistance (– · – ·) resulted in $R \propto \omega^{1.8}$ around 1 GHz, the measurements fit better to ω^2 (– – –). The solid curve, which fits the data over the entire range, is a calculation based on the smearing of the BCS density-of-states singularity by the energy gap anisotropy in the presence of impurity scattering [61]. The authors thank G. Müller for providing this figure.

Surface Resistance of Niobium

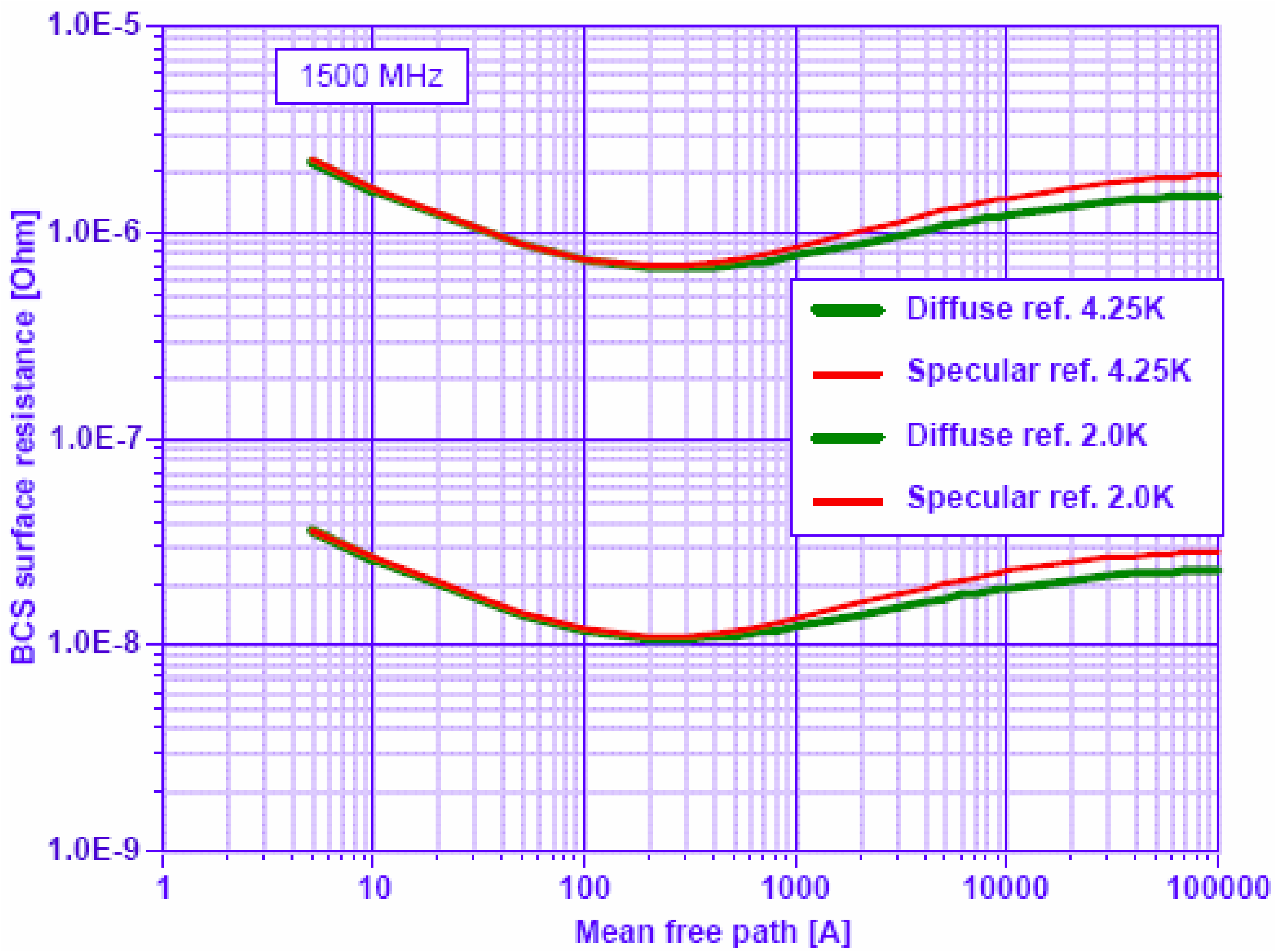

Super and Normal Conductors

- Normal Conductors
  - Skin depth proportional to $\omega^{-1/2}$
  - Surface resistance proportional to $\omega^{1/2}$
  - Surface resistance independent of temperature (at low T)
  - For Cu at 300K and 1 GHz, R_s=8.3 mΩ

- Superconductors
  - Penetration depth independent of ω
  - Surface resistance proportional to ω^2
  - Surface resistance strongly dependent of temperature
  - For Nb at 2 K and 1 GHz, R_s≈7 nΩ

However: do not forget Carnot

Accelerating Cavities

Two main functions

Mode transformer

$$\mathbf{TEM} \rightarrow \mathbf{TM}$$

Impedance transformer

$$\text{Low } Z \rightarrow \text{High } Z$$

Equivalent Circuit for an rf Cavity

Simple LC circuit representing
an accelerating resonator

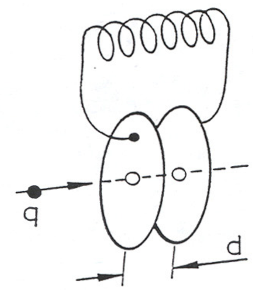

Simple lumped L-C circuit repesenting an accelerating resonator.
$\omega_o^2 = 1/LC$

Metamorphosis of the LC circuit
into an accelerating cavity

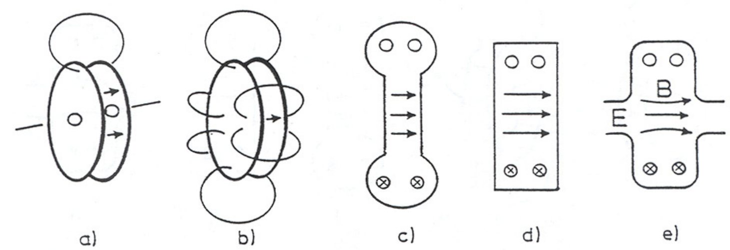

Metamorphosis of the L-C circuit of Fig. 1 into an accelerating cavity (after R.P.Feynman[33]). Fig. 5d shows the cylindrical "pillbox cavity" and Fig. 5e a slightly modified pillbox cavity with beam holes (typical β between 0.5 and 1.0). Fig. 5c resembles a low β version of the pillbox variety ($0.2<\beta<0.5$).

Chain of weakly coupled pillbox
cavities representing an accelerating
cavity

Chain of coupled pendula as
its mechanical analogue

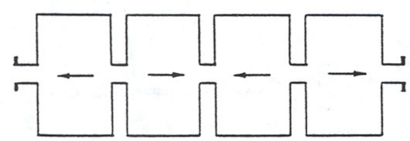

Chain of weakly-coupled pillbox cavities representing an accelerating module

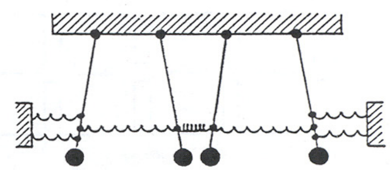

Chain of coupled pendula as a mechanical analogue to Fig. 6a

Design Considerations

$\dfrac{H_{s,\max}}{E_z}$	minimum	critical field
$\dfrac{E_{s,\max}}{E_z}$	minimum	field emission
$\dfrac{\langle \mathrm{H_s^2} \rangle}{E_z^2}$	minimum	shunt impedance, current losses
$\dfrac{\langle \mathrm{E_s^2} \rangle}{E_z^2}$	minimum	dielectric losses
$\dfrac{\mathrm{U}}{E_z^2}$	minimum maximum	control of microphonics voltage drop for high charge per bunch

RF Cavity Fundamental Quantities

- Quality Factor Q_0:

$$Q_0 \equiv \frac{\omega_0 U}{P_{diss}} = \frac{\text{Energy stored in cavity}}{\text{Energy dissipated in cavity walls per radian}} = \frac{\omega_0}{\Delta\omega_0} = \omega_0 \tau_0$$

- Shunt impedance R_{sh}: $R_{sh} \equiv \frac{V_c^2}{P_{diss}}$ in Ω

V_c = accelerating voltage

Note: Sometimes the shunt impedance is defined as $\frac{V_c^2}{2P_{diss}}$, or quoted as impedance per unit length (ohm/m)

Q – Geometrical Factor (Q R_s)

$$Q:\quad \frac{\text{Energy content}}{\text{Energy disspated during one radian}} = \omega\frac{U}{P} = \omega\tau = \frac{\omega}{\Delta\omega}$$

Rough estimate (factor of 2) for fundamental mode

$$\omega = \frac{2\pi c}{\lambda} \simeq \frac{2\pi}{\sqrt{\varepsilon_0\mu_0}}\frac{1}{2L} \qquad U = \frac{\mu_0}{2}\int H^2 dv \simeq \frac{\mu_0}{2}\frac{1}{2}H_0^2\frac{\pi L^3}{6}$$

$$P = \frac{1}{2}R_s\int H^2 dA = \frac{1}{2}R_s\frac{1}{2}H_0^2\,\pi L^2$$

$$QR_s \sim \frac{\pi}{6}\sqrt{\frac{\mu_0}{\varepsilon_0}} = 200\Omega$$

$G = QR_s$ is size (frequency) and material independent.

It depends only on the mode geometry

It is independent of number of cells

For superconducting elliptical cavities $QR_s \sim 275\Omega$

Shunt Impedance (R_{sh}), R_{sh} R_s, R/Q

$$R_{sh} = \frac{V^2}{P} \simeq \frac{E_z^2 L^2}{\frac{1}{2} R_s H_0^2 \pi L^2 \frac{1}{2}}$$

In practice for elliptical cavities

$$R_{sh} R_s \simeq 33{,}000 \ \left(\Omega^2\right) \text{ per cell}$$

$$R_{sh} / Q \simeq 100\Omega \text{ per cell}$$

$R_{sh}\,R_s$ and R_{sh}/Q

Independent of size (frequency) and material

Depends on mode geometry

Proportional to number of cells

Power Dissipated per Unit Length or Unit Area

$$\frac{P}{L} \propto \frac{1}{\frac{R}{Q} QR_S} \frac{E^2 R_S}{\omega}$$

For normal conductors $\qquad R_S \propto \omega^{1/2}$

$$\frac{P}{L} \propto \omega^{-\frac{1}{2}}$$

$$\frac{P}{A} \propto \omega^{\frac{1}{2}}$$

For superconductors $\qquad R_S \propto \omega^2$

$$\frac{P}{L} \propto \omega$$

$$\frac{P}{A} \propto \omega^2$$

Ponderomotive Effects and Microphonics

- Ponderomotive effects: changes in frequency caused by the electromagnetic field (radiation pressure)
  - Static Lorentz detuning (cw operation)
  - Dynamic Lorentz detuning (pulsed operation)

- Microphonics: changes in frequency caused by connections to the external world
  - Vibrations
  - Pressure fluctuations

Note: The two are not completely independent.

When phase and amplitude feedbacks are active, ponderomotive effects can change the response to external disturbances

Lorentz Detuning

- RF power produces radiation pressure: $P = (\mu_0 H^2 - \varepsilon_0 E^2)/4$
- Deformation produce a frequency shift:

$\Delta f = KL{*}E^2_{acc}$

Pressure deforms the cavity wall:

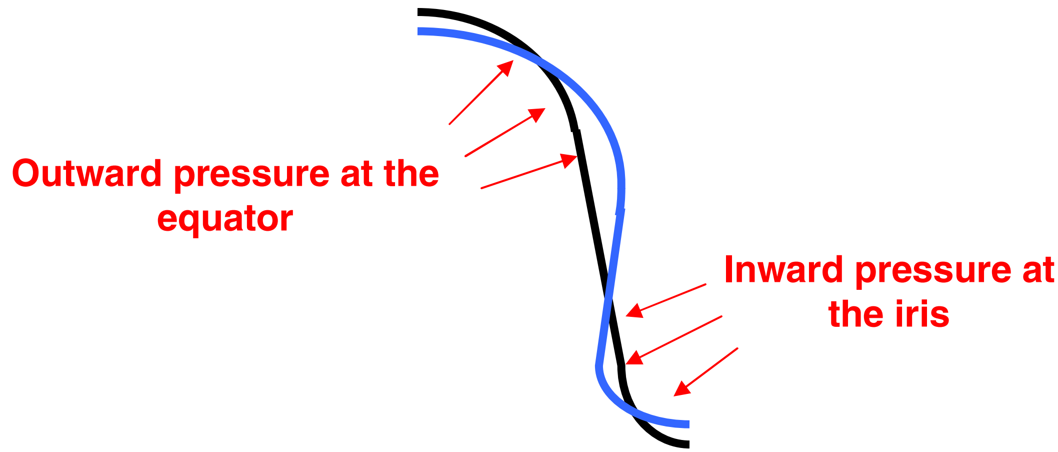

Lorentz Detuning

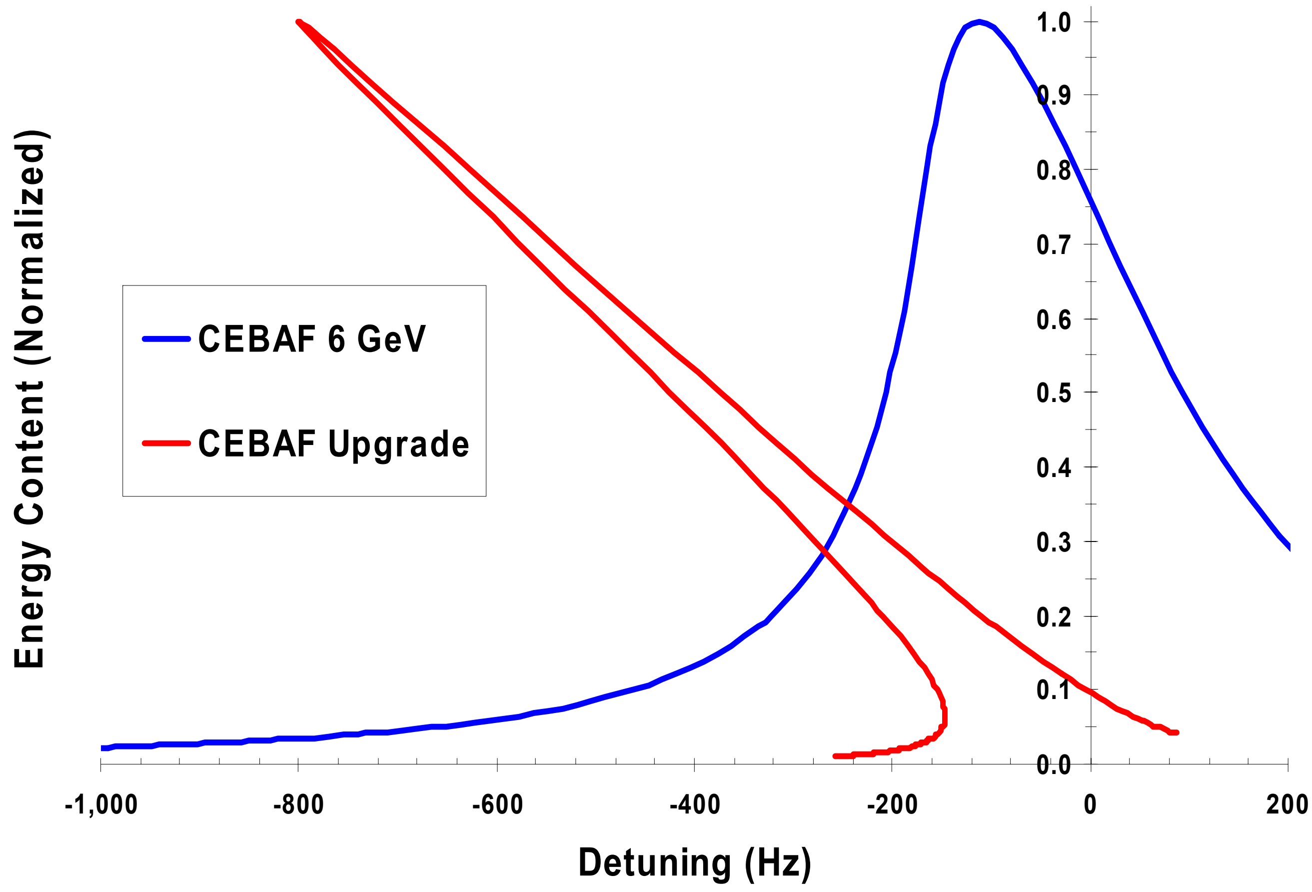

Microphonics

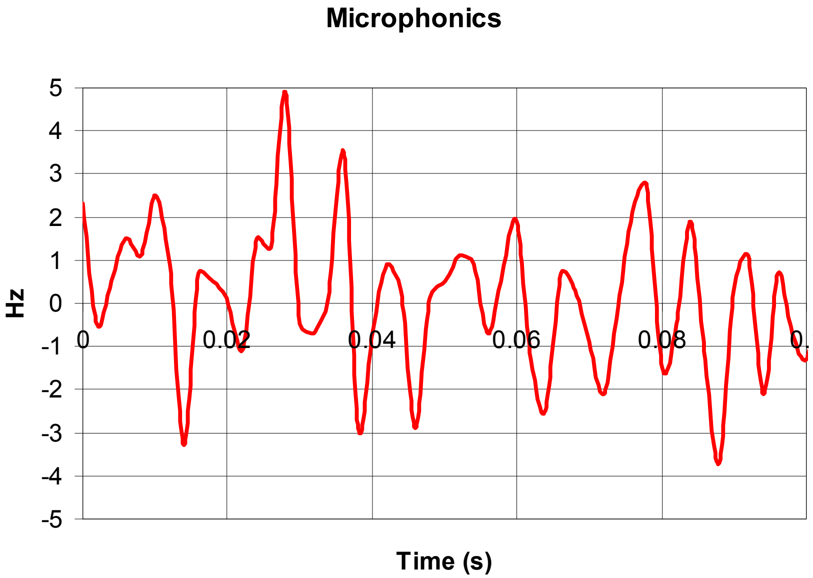

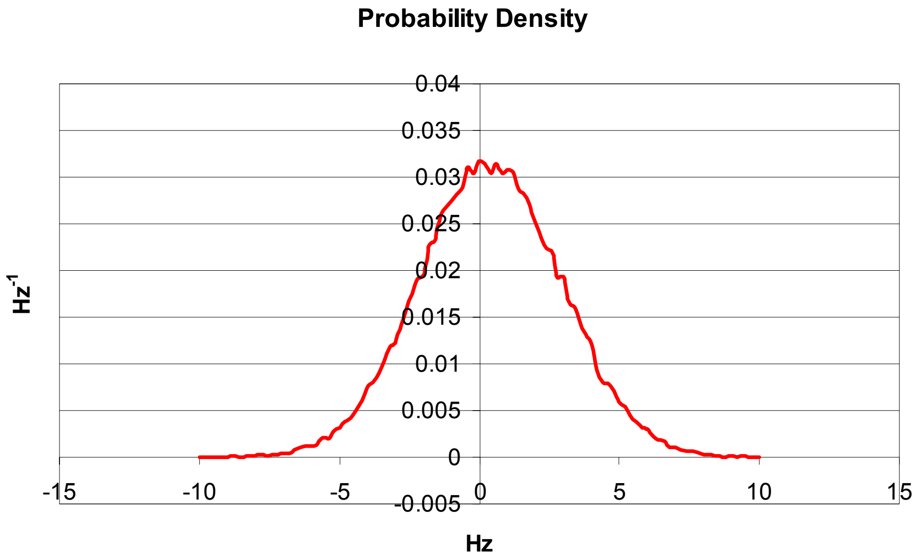

Limitations on the Performance of Superconducting Cavities

- Quenches below critical field
- Residual surface resistance
- Field emission
- Multipacting

- Causes
  - Surface contamination
  - Surface oxides
  - Defects
  - Grain boundaries

Parting Words

- SRF for accelerators has been an active area of research and development for 40 years
- Much progress has been done
- Many machines have been successfully built and operated
- We have not yet achieved the full potential of the “easiest” superconductor for rf applications (Nb)

Parting Words

- SRF involves many areas of physics and engineering
  - Quantum mechanics, solid state physics
  - Electromagnetism
  - Materials science, thin films, deposition techniques
  - Surface physics
  - Chemistry and electrochemistry
  - Vacuum science
  - Contamination control
  - Feedback systems and rf control
  - Cryogenics
  - Mechanical and thermal engineering

- There is plenty left to do